

Supplementary Material for

Particle Mass Yield from β -Caryophyllene Ozonolysis

Qi Chen¹, Yongjie Li^{1,2}, Karena A. McKinney³, Mikiyori Kuwata¹, and Scot T. Martin^{1,4,*}

[1] School of Engineering and Applied Sciences, Harvard University, Cambridge, Massachusetts, USA

[2] Division of Environment, Hong Kong University of Science and Technology, Hong Kong, China

[3] Department of Chemistry, Amherst College, Amherst, Massachusetts, USA

[4] Department of Earth and Planetary Sciences, Harvard University, Cambridge, Massachusetts, USA

Correspondence to: S.T. Martin (scot_martin@harvard.edu)

A. Wall-loss correction in a continuously mixed flow reactor (CMFR)

The mass balance of organic aerosol in a CMFR is described by the following equation:

$$\frac{dM_{\text{org, CMFR}}}{dt} = \frac{M_{\text{org, inflow}}}{\tau_{\text{CMFR}}} - \frac{M_{\text{org, CMFR}}}{\tau_{\text{CMFR}}} + F_{\text{org}} - \beta M_{\text{org, CMFR}} \quad (\text{A1})$$

where $M_{\text{org, CMFR}}$, $M_{\text{org, inflow}}$, τ_{CMFR} , F_{org} , and β represent the particle organic mass concentration in the CMFR ($\mu\text{g m}^{-3}$), the particle organic mass concentration in the inflow ($\mu\text{g m}^{-3}$), the mean residence time of the CMFR (s), the production rate of particle-phase organic material ($\mu\text{g m}^{-3} \text{ s}^{-1}$), and the assumed first-order particle wall-loss coefficient (s^{-1}), respectively. In our experiments, $M_{\text{org, inflow}} = 0$. At steady state,

$\frac{dM_{\text{org, CMFR}}}{dt} = 0$ and $M_{\text{org, CMFR}} = M_{\text{org, ss}}$. Equation A1 then becomes:

$$F_{\text{org}} = M_{\text{org, ss}} \left(\frac{1}{\tau_{\text{CMFR}}} + \beta \right) \quad (\text{A2})$$

At $\beta = 0$ (i.e., no particle wall loss),

$$F_{\text{org}}^{\beta=0} = M_{\text{org, ss}}^{\beta=0} \frac{1}{\tau_{\text{CMFR}}} \quad (\text{A3})$$

As discussed in Section 2.1, F_{org} is constant under different wall-loss conditions at steady state. The solution for Equations A2 and A3 is as follows:

$$M_{\text{org, ss}}^{\beta=0} = (1 + \beta\tau_{\text{CMFR}}) M_{\text{org, ss}} \quad (\text{A4})$$

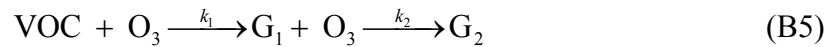
$M_{\text{org, ss}}^{\beta=0}$ is the organic mass concentration corrected by wall losses.

Gas-wall partitioning represents the net process of the re-evaporation of secondary organic material deposited on the walls and the absorption or reactive uptake of molecules from the gas phase, as well as direct deposition of particles to the walls.

This re-partitioning affects the gas-phase concentration of condensable species and hence the gas-phase chemistry as well as the gas-particle partitioning. Matsunaga and Ziemann (2010) showed that the gas-wall partitioning of various organic compounds was nearly independent of bag conditions and reversible, achieving equilibrium with time constants typically under one hour. For the 12-hour transient period used in our CMFR experiments, the surface layers of the Teflon bag material can be anticipated to become saturated, including the pore spaces near the surface. The non-reactive processes on the wall are expected to be in dynamic equilibrium with the CMFR at steady state, and depositing aerosol particles and the organic film on the walls can be supposed to have nearly identical compositions. Any reactive wall losses should then mimic any heterogeneous uptake on the suspended particles inside the bag.

B. β -Caryophyllene dark ozonolysis in a continuously mixed flow reactor (CMFR)

Based on the reaction rate constants of k_1 and k_2 , a simplified gas-phase reaction scheme for the β -caryophyllene ozonolysis can be described as:



where VOC, G_1 , and G_2 represent the precursor volatile organic compound, the first-generation products, and the second-generation products, respectively. Under an assumption of negligible wall losses of gas-phase species, the three differential equations that govern the species concentrations inside the CMFR are as follows:

$$\frac{d[\text{VOC}]}{dt} = \frac{[\text{VOC}]_0}{\tau} - \frac{[\text{VOC}]}{\tau} - k_1[\text{O}_3][\text{VOC}] \quad (\text{B6})$$

$$\frac{d[\text{G}_1]}{dt} = -\frac{[\text{G}_1]}{\tau} + k_1[\text{O}_3][\text{VOC}] - k_2[\text{O}_3][\text{G}_1] \quad (\text{B7})$$

$$\frac{d[G_2]}{dt} = -\frac{[G_2]}{\tau} + k_2[O_3][G_1] \quad (B8)$$

where τ is the residence time of the CMFR, $[VOC]_0$ is the concentration of β -caryophyllene in the CMFR inflow, $[O_3]$ is the ozone concentration, and $[VOC]$, $[G_1]$, and $[G_2]$ are the species concentrations in the CMFR outflow.

At steady state, $\frac{d[VOC]}{dt} = \frac{d[G_1]}{dt} = \frac{d[G_2]}{dt} = 0$. The algebraic solution for

Equations B2 to B4 are as follows:

$$[VOC]_{ss} = \frac{[VOC]_0}{\tau k_1 [O_3]_{ss} + 1} \quad (B9)$$

$$[G_1]_{ss} = \frac{\tau k_1 [O_3]_{ss} [VOC]_0}{(\tau k_1 [O_3]_{ss} + 1)(\tau k_2 [O_3]_{ss} + 1)} \quad (B10)$$

$$[G_2]_{ss} = \frac{\tau^2 k_1 k_2 [O_3]_{ss}^2 [VOC]_0}{(\tau k_1 [O_3]_{ss} + 1)(\tau k_2 [O_3]_{ss} + 1)} \quad (B11)$$

The ozone concentration was maintained at steady state in the CMFR for each experiment. The reaction rate constants are 1.16×10^{-14} molecule⁻¹ cm³ s⁻¹ for the ozonolysis of the endo-cyclic double bond (k_1) of β -caryophyllene (Shu and Atkinson, 1995) and 1.1×10^{-16} molecule⁻¹ cm³ s⁻¹ for the ozonolysis of the exo-cyclic double bond (k_2) of the first generation products (Winterhalter et al., 2009). The mean residence time of the chamber is 13000 s.

C. Parameters used in air quality models

Regional and global chemical transport models have employed parameterizations derived from the data reported by Griffin et al. (1999) to estimate the contribution of sesquiterpenes to the ambient organic particle mass concentrations (Chung and Seinfeld,

2002; Sakulyanontvittaya et al., 2008; Carlton et al., 2010; Zhang and Ying, 2011). Table S2 listed the parameters used in Goddard Institute for Space Studies General Circulation Model II-prime (GISS GCM II-prime) and Community Multiscale Air Quality Model (CMAQ). The mass-based stoichiometric yield α and the product saturation concentration C^* were derived for one-product model (Odum et al., 1996; Kroll and Seinfeld, 2008) as described as follows:

$$Y(M_{\text{org}}) = \alpha \left(1 + \frac{C^*}{M_{\text{org}}} \right)^{-1} \quad (\text{C1})$$

where Y is the particle mass yield and M_{org} is the organic mass concentration. The gas-to-particle partitioning of semivolatile compounds depends on temperature. C^* is therefore defined by the Clausius-Clapeyron equation as follows:

$$C^*(T) = C^*(T_0) \frac{T_0}{T} \exp \left[\frac{\Delta H_{\text{vap}}}{R} \left(\frac{1}{T_0} - \frac{1}{T} \right) \right] \quad (\text{C2})$$

where ΔH_{vap} is the vaporization enthalpy, R is the ideal gas constant, and T_0 is the reference temperature (i.e., 308 K for β -caryophyllene oxidation in Griffin et al. (1999)). Recent experimental data suggest that the ΔH_{vap} values used in earlier versions of CMAQ ($\Delta H_{\text{vap}} = 156$ or 163 kJ mol^{-1} in version 4.3 to 4.6) were overestimates (Offenberg et al., 2006). The new ΔH_{vap} value of 40 kJ mol^{-1} was used in CMAQ version 4.7 (Carlton et al., 2010; Zhang and Ying, 2011).

The original analysis of Griffin et al. (1999) assumed a density of 1000 kg m^{-3} for secondary organic material (SOM), which was adapted by Chung and Seinfeld (2002) and Sakulyanontvittaya et al. (2008) in their models. The original CMAQ v4.7 (Zhang and Ying, 2011) scaled the values of α by 30% to account for recent laboratory

measurements of density of 1300 kg m^{-3} for β -caryophyllene-derived SOM (Bahreini et al., 2005). More accurately, Carlton et al. (2010) derived a new set of α and C^* from the original data from Griffin et al. (1999) in which both Y and M_{org} were corrected by the SOM density of 1300 kg m^{-3} and the data from Hoffmann et al. (1997) were excluded.

The parameters for β -caryophyllene (Table S2) were used for all sesquiterpenes when estimating sesquiterpene-derived particle mass concentrations in Sakulyanontvittaya et al. (2008). In CMAQ v4.7 (original and revised) and GISS GCM II-prime, the parameters for both β -caryophyllene and α -humulene oxidation were lumped together to represent the overall sesquiterpene oxidation.

Excess Ozone (ppbv)	α_0	α_1	α_2
50	0.15 ± 0.02	0.16 ± 0.07	0.32 ± 0.13
100	0.13 ± 0.03	0.22 ± 0.10	0.38 ± 0.15
200	0.17 ± 0.05	0.11 ± 0.17	1.03 ± 0.30

Table S1. Summary of the optimized mass-based stoichiometric yields α_i of product class i for β -caryophyllene ozonolysis. The volatility of product class i is prescribed in decadal units of 10^{-i} , where 10^{-i} is denoted as C_i^* .

Reference	Model	α	C^* at 298 K ($\mu\text{g m}^{-3}$)	C^* at 308 K ($\mu\text{g m}^{-3}$)	ΔH_{vap} (kJ mol^{-1})
Chung et al. (2002)	GISS GCM II-prime	1.000	14.329	24.039	42
Sakulyanontvittaya et al. (2008)	CMAQ v4.5	1.000	2.935	24.039	163
Zhang et al. (2011)	CMAQ original v4.7	1.300	14.710	24.039	40
Carlton et al. (2010) (cf. Table S-1)	CMAQ revised v4.7	1.537	29.893	48.852	40

Table S2. Summary of the mass-based stoichiometric yield α , the product saturation concentration C^* , and the vaporization enthalpy ΔH_{vap} used in four different regional and global models for β -caryophyllene oxidation. Parameters were derived for one-product model (Eq. C1) based on the yield data (or partially data) reported by Griffin et al. (1999) for β -caryophyllene photooxidation at 308 K.

List of Figures

- Figure S1.** Two examples of the mass-diameter distributions recorded by the AMS compared to the distributions calculated from the number-diameter SMPS measurements and an optimized particle effective density ρ_{eff} .
- Figure S2.** Scatter plot of the total particle mass concentrations measured by the AMS and the mass concentrations calculated from the SMPS data using the optimized particle effective densities of each experiment. Error boxes around the data points show the instrument uncertainty of 30% for the AMS (Jimenez et al., 2003) and the SMPS (Wiedensohler et al., 2010).
- Figure S3.** Dependence of the material density ρ_{org} of the particle-phase organic material on the wall-loss corrected organic particle mass concentration $M_{\text{org,corr}}$. Results are shown for both the DMA-APM and the AMS-SMPS methods.
- Figure S4.** (a) Differential and (b) cumulative number-diameter distributions of the SOM-coated sulfate particles for the experiments of Table 2.
- Figure S5.** Particle mass yield before and after applying wall-loss corrections (Equation 1). Black dots represent a subset of the data collected under typical wall-loss conditions ($\beta = 1.04 \pm 0.11 \text{ h}^{-1}$) (Table 2). Red dots represent data collected for modified wall-loss conditions ($\beta = 0.19 \pm 0.02 \text{ h}^{-1}$ for Exp. #27 in panel a1/a2) and ($\beta = 0.49 \pm 0.03 \text{ h}^{-1}$ for Exp. #10 in panel b1/b2). Solid lines are drawn to guide the eye.
- Figure S6.** Chemical structures associated with product labeling used in the main text and highlighting ozonolytic conversions from first- to second-generation

products. The conversions from first- to second-generation products are presented by arrows. The red label calls attention to a product that appears to have been incorrectly assigned in previous work (Li et al., 2011).

Literature Cited

- Bahreini, R., Keywood, M. D., Ng, N. L., Varutbangkul, V., Gao, S., Flagan, R. C., Seinfeld, J. H., Worsnop, D. R., and Jimenez, J. L.: Measurements of secondary organic aerosol from oxidation of cycloalkenes, terpenes, and m-xylene using an Aerodyne aerosol mass spectrometer, *Environ. Sci. Technol.*, 39, 5674-5688, doi:10.1021/es048061a, 2005.
- Carlton, A. G., Bhave, P. V., Napelenok, S. L., Edney, E. D., Sarwar, G., Pinder, R. W., Pouliot, G. A., and Houyoux, M.: Model Representation of Secondary Organic Aerosol in CMAQv4.7, *Environ. Sci. Technol.*, 44, 8553-8560, doi:10.1021/es100636q, 2010.
- Chung, S. H., and Seinfeld, J. H.: Global distribution and climate forcing of carbonaceous aerosols, *J. Geophys. Res.*, 107, 4407, doi:10.1029/2001jd001397, 2002.
- Griffin, R. J., Cocker, D. R., Flagan, R. C., and Seinfeld, J. H.: Organic aerosol formation from the oxidation of biogenic hydrocarbons, *J. Geophys. Res.*, 104, 3555-3567, 1999.
- Hoffmann, T., Odum, J. R., Bowman, F., Collins, D., Klockow, D., Flagan, R. C., and Seinfeld, J. H.: Formation of organic aerosols from the oxidation of biogenic hydrocarbons, *J. Atmos. Chem.*, 26, 189-222, 1997.
- Jimenez, J. L., Jayne, J. T., Shi, Q., Kolb, C. E., Worsnop, D. R., Yourshaw, I., Seinfeld, J. H., Flagan, R. C., Zhang, X. F., Smith, K. A., Morris, J. W., and Davidovits, P.: Ambient aerosol sampling using the Aerodyne Aerosol Mass Spectrometer, *J. Geophys. Res.*, 108, 8425, doi:10.1029/2001jd001213, 2003.
- Kroll, J. H., and Seinfeld, J. H.: Chemistry of secondary organic aerosol: Formation and evolution of low-volatility organics in the atmosphere, *Atmos. Environ.*, 42, 3593-3624, doi:10.1016/j.atmosenv.2008.01.003, 2008.
- Li, Y. J., Chen, Q., Guzman, M. I., Chan, C. K., and Martin, S. T.: Second-generation products contribute substantially to the particle-phase organic material produced by β -caryophyllene ozonolysis, *Atmos. Chem. Phys.*, 11, 121-132, doi:10.5194/acp-10-1-2010, 2011.
- Matsunaga, A., and Ziemann, P. J.: Gas-wall partitioning of organic compounds in a Teflon film chamber and potential effects on reaction product and aerosol yield measurements, *Aerosol Sci. Technol.*, 44, 881-892, doi:10.1080/02786826.2010.501044, 2010.
- Odum, J. R., Hoffmann, T., Bowman, F., Collins, D., Flagan, R. C., and Seinfeld, J. H.: Gas/particle partitioning and secondary organic aerosol yields, *Environ. Sci. Technol.*, 30, 2580-2585, 1996.
- Offenberg, J. H., Kleindienst, T. E., Jaoui, M., Lewandowski, M., and Edney, E. O.: Thermal properties of secondary organic aerosols, *Geophys. Res. Lett.*, 33, L03816, doi:10.1029/2005gl024623, 2006.

Sakulyanontvittaya, T., Guenther, A., Helmig, D., Milford, J., and Wiedinmyer, C.: Secondary organic aerosol from sesquiterpene and monoterpene emissions in the United States, *Environ. Sci. Technol.*, 42, 8784-8790, doi:10.1021/es800817r, 2008.

Shu, Y. H., and Atkinson, R.: Atmospheric lifetimes and fates of a series of sesquiterpenes, *J. Geophys. Res.*, 100, 7275-7281, doi:10.1029/95JD00368, 1995.

Wiedensohler, A., Birmili, W., Nowak, A., Sonntag, A., Weinhold, K., Merkel, M., Wehner, B., Tuch, T., Pfeifer, S., Fiebig, M., Fjåraa, A. M., Asmi, E., Sellegri, K., Depuy, R., Venzac, H., Villani, P., Laj, P., Aalto, P., Ogren, J. A., Swietlicki, E., Roldin, P., Williams, P., Quincey, P., Hüglin, C., Fierz-Schmidhauser, R., Gysel, M., Weingartner, E., Riccobono, F., Santos, S., Grüning, C., Faloon, K., Beddows, D., Harrison, R. M., Monahan, C., Jennings, S. G., O'Dowd, C. D., Marinoni, A., Horn, H. G., Keck, L., Jiang, J., Scheckman, J., McMurry, P. H., Deng, Z., Zhao, C. S., Moerman, M., Henzing, B., and de Leeuw, G.: Particle mobility size spectrometers: harmonization of technical standards and data structure to facilitate high quality long-term observations of atmospheric particle number size distributions, *Atmos. Meas. Tech. Discuss.*, 3, 5521-5587, doi:10.5194/amtd-3-5521-2010, 2010.

Winterhalter, R., Herrmann, F., Kanawati, B., Nguyen, T. L., Peeters, J., Vereecken, L., and Moortgat, G. K.: The gas-phase ozonolysis of β -caryophyllene ($C_{15}H_{24}$). Part I: an experimental study, *Phys. Chem. Chem. Phys.*, 11, 4152-4172, doi:10.1039/b817824k, 2009.

Zhang, H. L., and Ying, Q.: Secondary organic aerosol formation and source apportionment in Southeast Texas, *Atmos. Environ.*, 45, 3217-3227, doi:10.1016/j.atmosenv.2011.03.046, 2011.

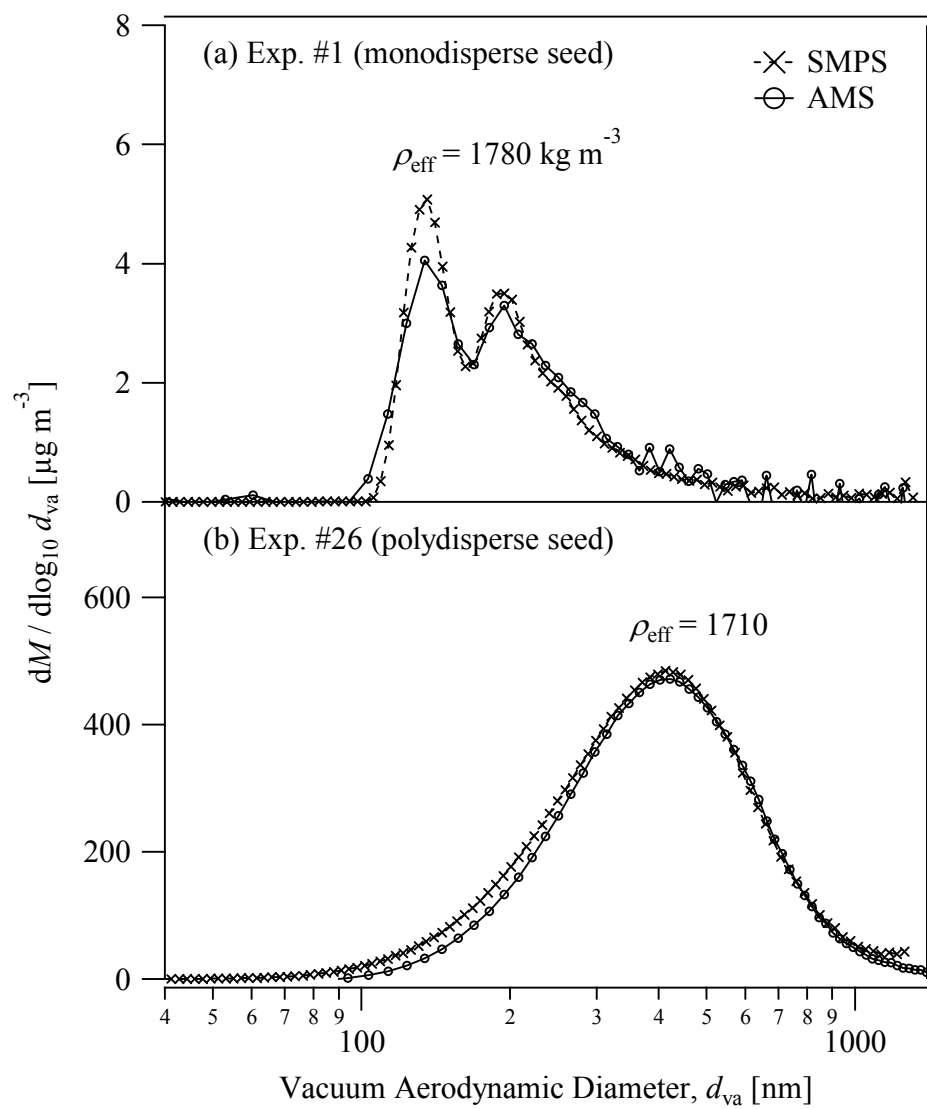


Figure S1

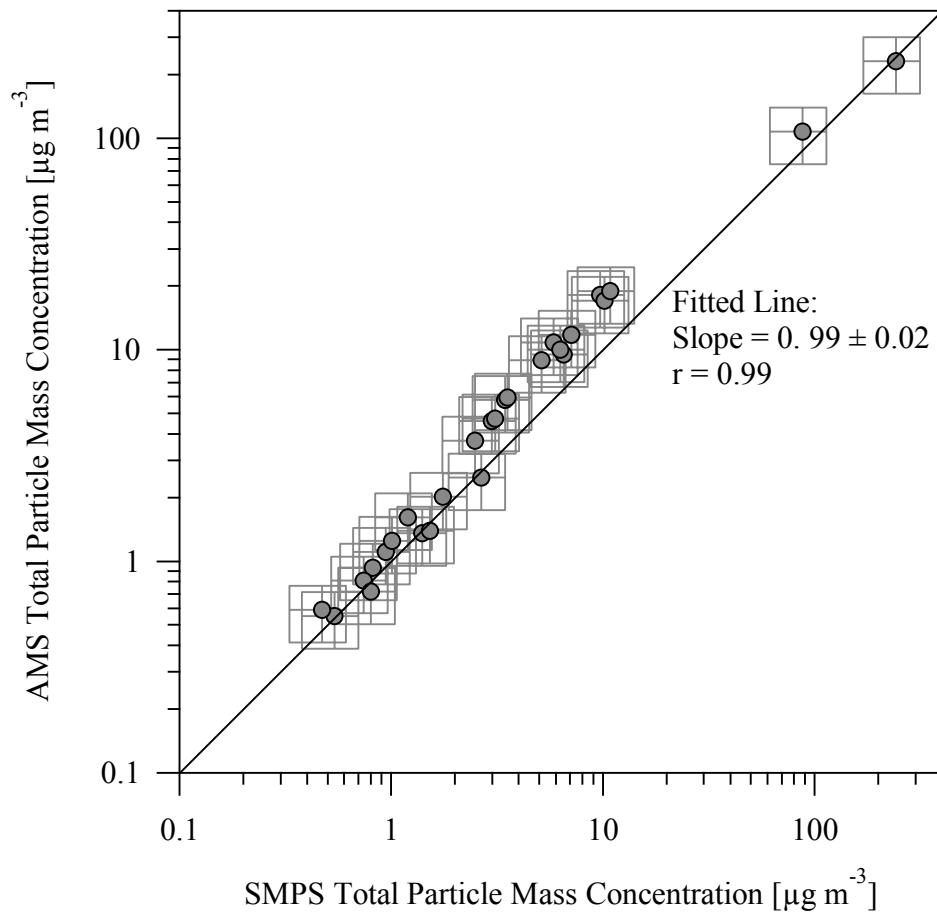


Figure S2

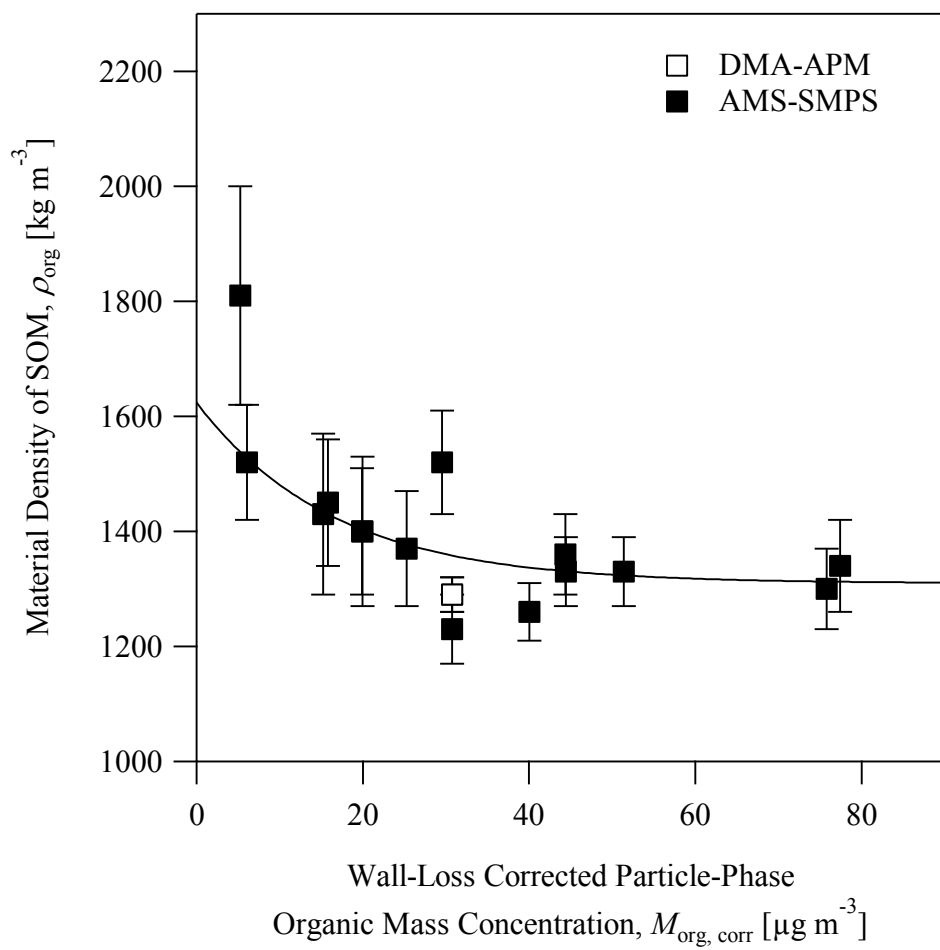


Figure S3

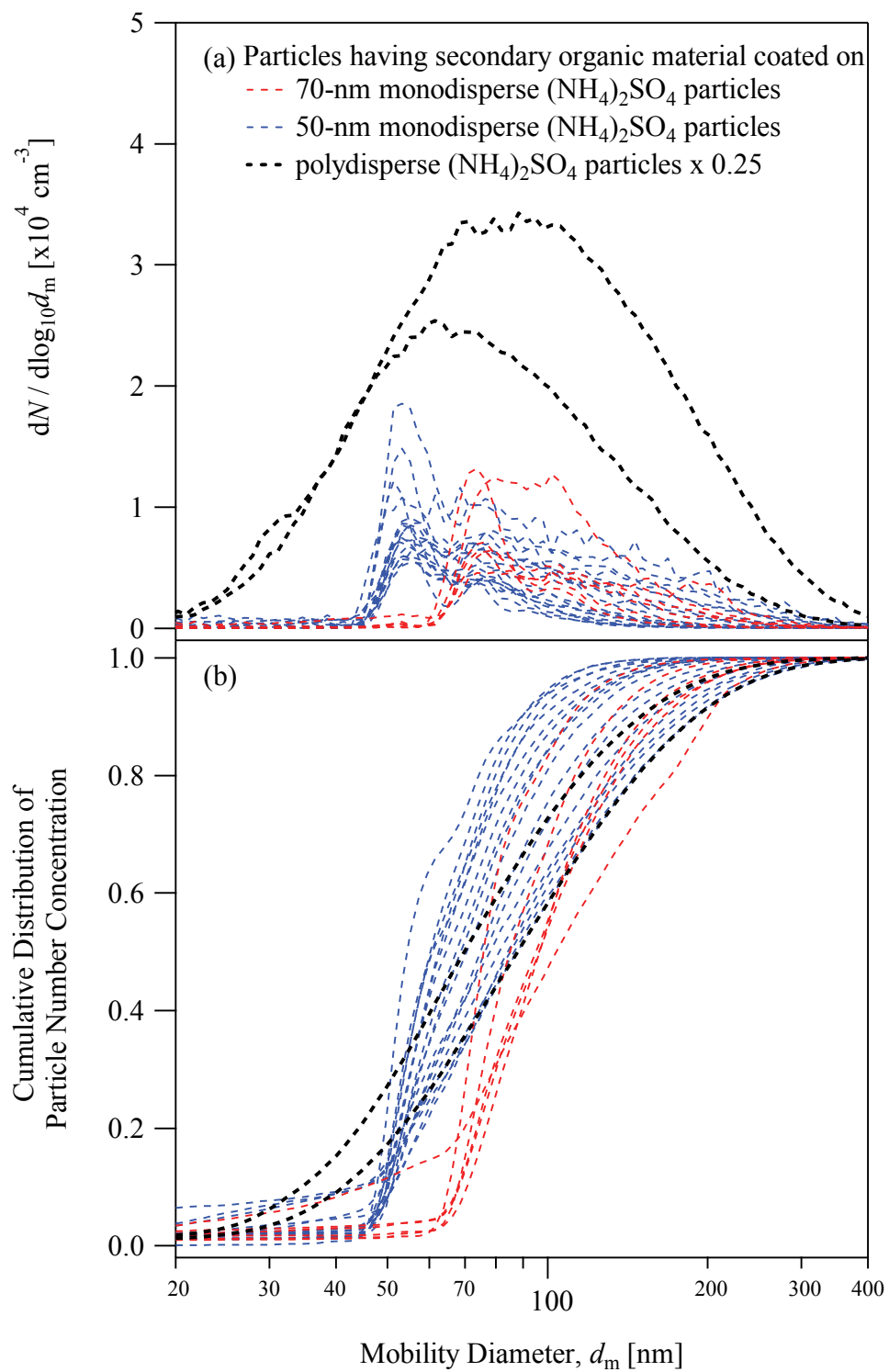


Figure S4

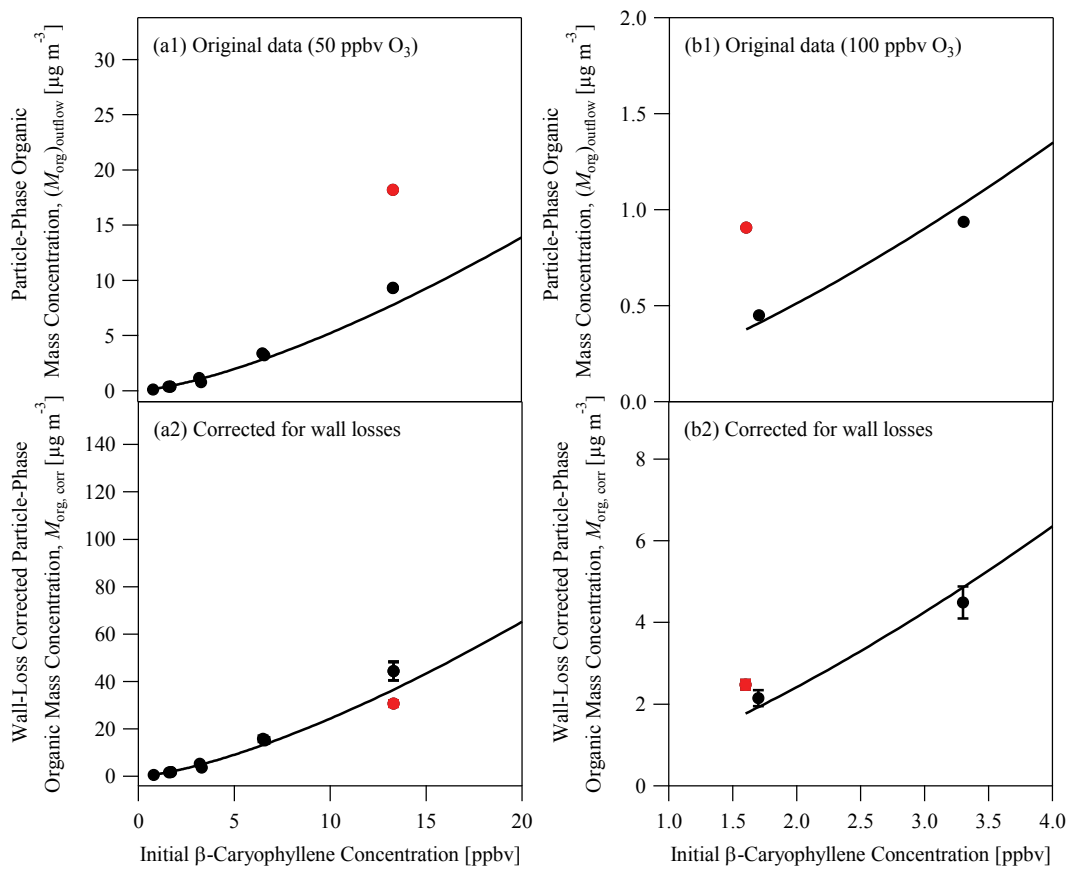


Figure S5

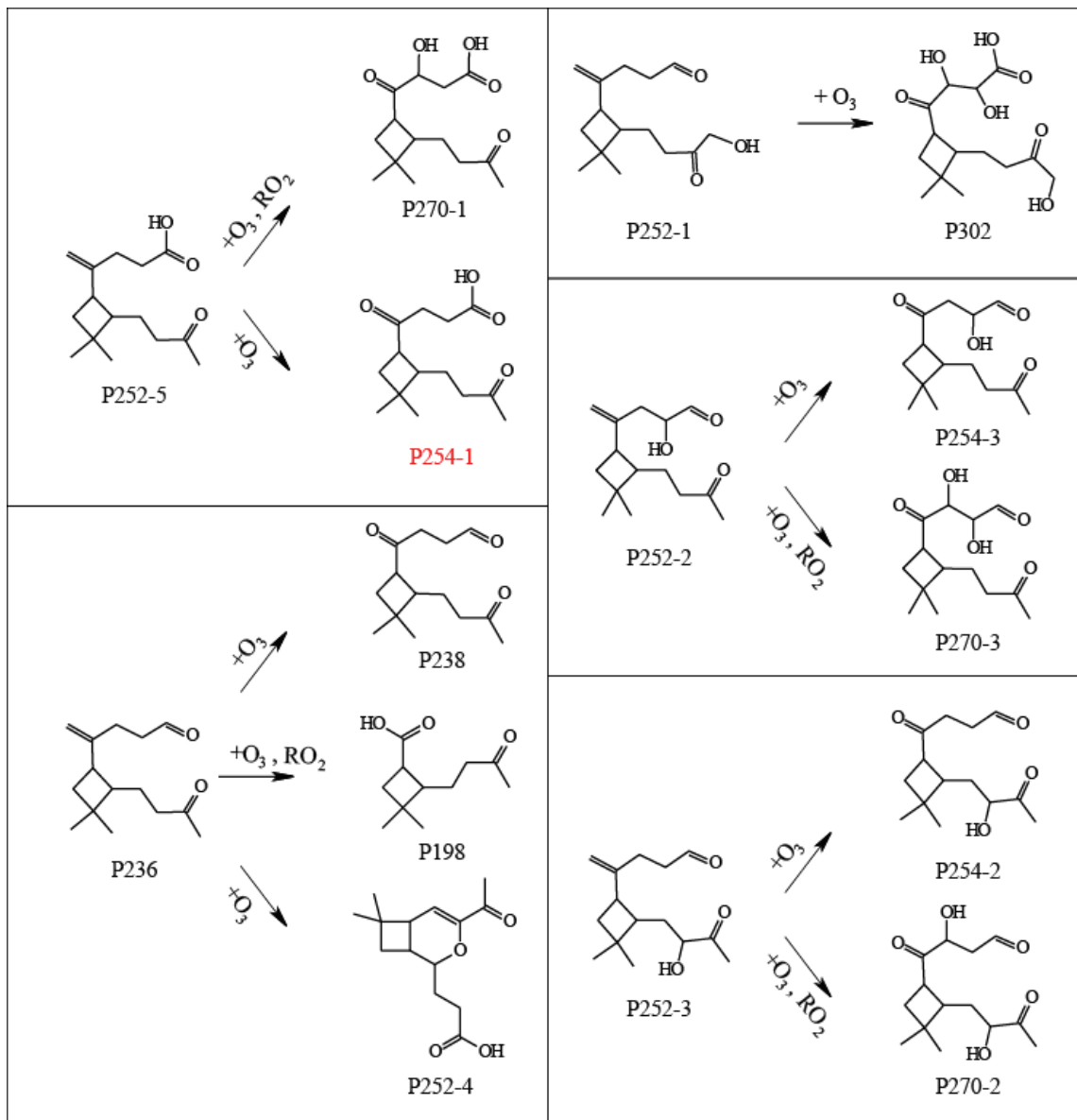


Figure S6